Vol. 694: 45–59, 2022
https://doi.org/10.3354/meps14107

MARINE ECOLOGY PROGRESS SERIES
Mar Ecol Prog Ser

Published August 11

Macrocystis pyrifera forest development shapes the physical environment through current velocity reduction

Kristen Elsmore[1,*], Kerry J. Nickols[2], Tom Ford[3], Katherine C. Cavanaugh[4], Kyle C. Cavanaugh[4], Brian Gaylord[1,5]

[1]Bodega Marine Laboratory, University of California, Davis, Bodega Bay, CA 94923, USA
[2]Department of Biology, California State University, Northridge, Northridge, CA 91330, USA
[3]Coastal Research Institute, Loyola Marymount University, Los Angeles, CA 90045, USA
[4]Department of Geography, University of California, Los Angeles, Los Angeles, CA 90095, USA
[5]Department of Evolution and Ecology, University of California, Davis, Davis, CA 95616, USA

ABSTRACT: Marine forests of the giant kelp *Macrocystis pyrifera* create biogenic habitat spanning the water column, within which hydrodynamic conditions can differ strongly from those outside. Such flow alteration has implications for physical, chemical, and ecological processes across multiple spatial scales. At the forest-wide scale, *M. pyrifera* has been shown to decrease alongshore current velocities, but relatively little is known about how the attenuation of such currents evolves as new kelp forests emerge and mature. Here, we quantified alongshore current velocities outside and within a temperate rocky reef environment that twice underwent a transition from a barren state to one in which a thick surface canopy was present. We identified a threshold density during forest emergence at which much of the attenuation of alongshore depth-averaged velocity occurs — 3 stipes m^{-2} with a surface canopy present. Incremental increases in damping occur as the forest matures, highlighting that relatively young, thin forests can induce substantially reduced flows. Additionally, the presence of a young forest's subsurface canopy and its subsequent increase in height create a seasonally changing profile of varying velocities through the water column. These results indicate greater complexity in how canopy-forming kelp influence nearshore flow properties than has often been recognized. Importantly, emerging forests can alter the nearshore environment through modulation of current speeds shortly following initial recruitment, with consequences for the transport of larvae, nutrients, and sediment throughout the forest and adjacent habitats.

KEY WORDS: Current velocity · *Macrocystis pyrifera* · Kelp forest · Nearshore hydrodynamics · Ecosystem service · Kelp restoration

1. INTRODUCTION

Currents play a critical role in shaping the biotic communities that inhabit coastal waters. Nearshore currents influence larval transport, dispersal, and retention patterns, which have consequences for the genetic structure and connectivity of marine populations (Gaylord & Gaines 2000, Siegel et al. 2003, 2008, Nickols et al. 2012, 2015, Morgan et al. 2018). They also play an important role in delivering nutrients to nearshore habitats, driving growth rates of both pelagic and habitat-forming primary producers (Hurd 2000, McPhee-Shaw et al. 2007, Fram et al. 2008, Gaylord et al. 2012). Furthermore, currents

*Corresponding author: keelsmore@ucdavis.edu

interact with waves and bottom topography to control particle suspension, deposition, and transport at the coastal edge (Gaylord et al. 2002, 2004). These and other interactions influence water clarity, benthic scouring, and reef burial, each of which has been shown to negatively impact benthic community members (Dayton et al. 1984, Watanabe et al. 2016).

Often referred to as an ecosystem engineer, the giant kelp *Macrocystis pyrifera* creates biogenic habitat spanning the benthos to the surface; its fronds consequently impose drag on currents throughout the water column. *M. pyrifera* has been shown to alter water movement at multiple spatial scales, with implications for physical, chemical, and ecological processes (Gaylord et al. 2012). Most notably, at the patch to forest-wide scale (100s to 1000s of m), *M. pyrifera* can dramatically decrease alongshore current velocities and, to a lesser degree, cross-shore current velocities (Jackson 1998, Gaylord et al. 2007, Rosman et al. 2007). Such modifications to flow not only have consequences for community residents but can result in bio-physical and bio-chemical feedbacks with the vegetation itself (Hurd 2000, Reed et al. 2006, Gaylord et al. 2012, Frieder et al. 2012, Koweek et al. 2017, Hirsh et al. 2020, Traiger et al. 2022). For example, maintenance of sufficient nutrients relies on the delivery of new, nitrate-replete water throughout the kelp forest. Reduced current velocities can impair such delivery, resulting in nutrient limitation that slows growth rates of the forest (Hurd 2000). Decreased cross-shore exchange, which can accompany reduced flows, further increases retention of nutrient-depleted waters, contributing to forest-wide senescence (Zimmerman & Kremer 1986, Rodriguez et al. 2013). Current velocities also influence vertical mixing, which affects kelp propagule sinking speeds and thus spore dispersal distances (Gaylord et al. 2002, 2006). Importantly, reduced current velocities result in shorter spore dispersal distances (Gaylord et al. 2004) which, in turn, can increase the potential for self-fertilization with associated reductions in fitness (Raimondi et al. 2004, Reed et al. 2006).

Within-forest flows can be slower than incident ones by an order of magnitude or more (Jackson 1998, Gaylord et al. 2007, Rosman et al. 2007). However, studies quantifying kelp-associated current modification have been limited mostly to week- to month-long examinations in particular seasons. Forest density and canopy cover do exhibit general seasonal trends, reaching their peak in the late summer months and their low in winter (Reed et al. 2009, Cavanaugh et al. 2011). Importantly, however, physical and biological processes can operate individually or in concert to drive more irregular patterns of kelp forest succession and, consequently, alter forest structure over a range of timescales (North 1971, Tegner et al. 1997, Graham et al. 2007, Rodriguez et al. 2013). The relative sparsity of longer-term hydrodynamic data gains even greater relevance given this dynamic character of *M. pyrifera* forests. A broader temporal understanding of kelp effects on flow is critical for determining long-term consequences for forest inhabitants, especially those that depend on water motion for the provision of food, for successful fertilization (as in broadcast spawners, where egg and sperm meet through mixing), and for delivery of larvae required to sustain populations.

Giant kelp beds experience large changes in density, areal coverage, and even height as new individuals emerge, add fronds (i.e. stipes with attached blades), and proliferate on the water's surface. The vertical distribution of kelp material within the water column (e.g. canopy height) inherently determines the profile of drag imposed on impinging currents and likely influences the spatial patterns of attenuation throughout the water column. Nevertheless, previous *in situ* efforts have neglected much of this complexity, while focusing largely on comparisons of depth-averaged current velocities. Although some work has compared near-surface and near-bottom flows, noting important seasonal differences in the velocity gradient throughout the water column (Gaylord et al. 2007, Rosman et al. 2007), understanding of finer details remains incomplete. This information gap creates uncertainties in attempts to understand processes associated with certain vertical regions within a kelp forest. For example, *M. pyrifera* spores are released in the lower portion of the water column where this species' reproductive sporophylls reside, while sites of nutrient uptake occur primarily at the photosynthetic blades which are populated throughout the water column but concentrated at the surface. In the nearshore environment, nutrient-replete waters are typically found near the benthos, below the thermocline (Konotchick et al. 2012). Gradients in the flow profile can influence vertical mixing between the upper and lower regions of the water column, affecting nutrient supply throughout the water column and uptake rates by *M. pyrifera* blades (Fram et al. 2008, Rosman et al. 2010, Konotchick et al. 2012, Kregting et al. 2011). Detailed investigations of vertical velocity gradients within kelp forests are therefore warranted.

Given *M. pyrifera*'s well-documented capacity to substantially attenuate alongshore currents (more so than those in the cross-shore direction), this study focused on understanding the evolution of along-

shore current attenuation throughout forest maturation. Here, we quantified current velocities outside and within a temperate rocky reef that twice underwent a transition from a barren state, in which the habitat was devoid of any vegetation, to one in which a thick surface canopy was present. Through this experimental framework, we address 2 specific questions: (1) to what extent does attenuation of alongshore current velocities depend on forest age as forest characteristics (stipe density, individual density, number of stipes per individual, and surface canopy cover) change during forest development and (2) to what extent does alongshore current attenuation differ throughout the water column as a subsurface canopy emerges and develops into a surface canopy?

2. MATERIALS AND METHODS

2.1. Study site

The focal site for this study, Marguerite Reef (33.757° N, 118.418° W), sits along the Palos Verdes Peninsula, within the central region of the Southern California Bight (Fig. 1), near Los Angeles, California, USA. The site is positioned along a roughly linear stretch of coastline, with a shoreline angle of 340° from north. In this region, subtidal currents are generally along-isobath with amplitudes of 10–20 cm s^{-1} (Noble et al. 2009). Substrate at Marguerite Reef is composed of bedrock and large boulders interspersed with sand patches. Prior to this study, the reef was dominated by purple urchins *Strongylocentrotus purpuratus*, which were sufficiently abundant that the system had shifted into a 'barren' state with little to no macrophytes present (Burdick et al. 2016). As part of a broader kelp restoration project, the purple urchins were culled from Marguerite Reef between August 2016 and January 2017, and a *Macrocystis pyrifera* forest subsequently developed, with kelp recruits observed on the seafloor as early as March 2017. There was little-to-no understory algal community present throughout the study (Panos 2022), with a sparse and transient appearance of algal individuals across the site, including solitary individuals of *Sargassum horneri*, *S. muticum*, *Pterygophora californica*, *Eisenia arborea*, and *Egregia menziesii* (Grime et al. 2020). Purple urchin densities remained below 2 m^{-2} throughout the duration of this study (Grime et al. 2020). Coincident with high sea surface temperatures and elevated turbidity due to a nearby landslide, the kelp forest again disappeared in December 2018 but began to re-emerge in June 2019. These changes in kelp density allowed for an exploration of forest effects on currents spanning 2 full cycles of kelp recovery and regrowth.

2.2. Kelp forest dynamics

A combination of subtidal SCUBA surveys and satellite imagery was used to quantify changes in *M. pyrifera* forest structure throughout the study. Monthly subtidal swath surveys were conducted by divers over 2 experimental periods: November 2016–May 2018 and April 2019–October 2019, referenced as the 2017 and 2019 experiments, respectively. Between November 2016 and May 2018, surveys were conducted along 8 evenly spaced transects (30 × 4 m,

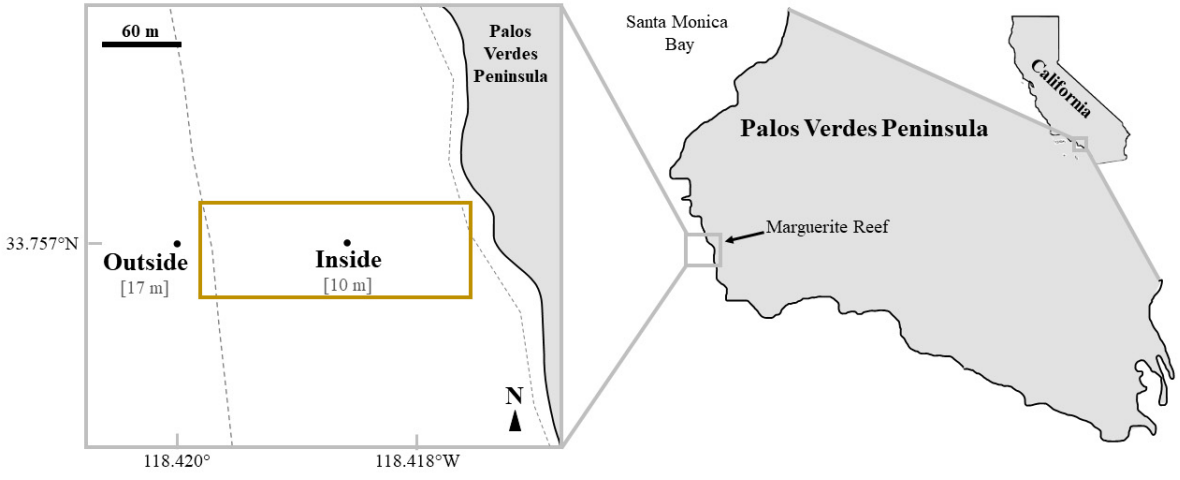

Fig. 1. Marguerite Reef, Palos Verdes, California, USA, showing locations of the instruments placed inside and outside reef habitat (black dots); mean depths are noted within brackets. Dashed lines: outer and inner edges of the kelp forest, which generally follow seabed isobaths; yellow box: spatial extent within which kelp parameters were quantified

30 m apart), positioned along a reference line oriented perpendicular to shore (Fig. 1). Each individual transect ran parallel to shore. From April 2019 to October 2019, the 8 transects had dimensions of 30 × 2 m but otherwise followed the same sampling protocol. Along each transect, *M. pyrifera* individuals taller than 1 m and their respective stipes were counted to estimate the density of giant kelp. Observations of plant heights were recorded within 10 × 2 m sections of each transect to assess the rapidly changing subsurface canopy height as the *M. pyrifera* forest developed. These observations included the presence of individuals less than 1 m tall to capture the onset of new forest development.

Surface canopy extents were derived from high-resolution PlanetScope satellite data covering the boundary of the subtidal survey area (Fig. 1). An average of 5 images mo^{-1} were collected between November 2016 and December 2019. PlanetScope images are 3 m resolution, contain 4 spectral bands (red, green, blue, and near-infrared), and are atmospherically and geometrically corrected (Planet 2021). All images were manually digitized into 2 classes ('kelp' and 'other') using ArcGIS software (ESRI). Monthly composites were created by calculating the class with the maximum number of observations within a single month for each pixel (i.e. if a pixel was classified as kelp canopy in 3 of the 5 images for that month, it was considered kelp canopy). This compositing helped account for errors in classification of individual images. To acquire the percentage of canopy cover that overlapped spatially with the subtidal kelp surveys, the maximum monthly coverage of surface canopy, determined by the monthly compositing, was then divided by the total boxed survey area (14 850 m^2; Fig. 1).

2.3. Alongshore current velocity measurements

Water velocities along 3 axes (east, north, and up [ENU] coordinates) were measured outside (depth 17 ± 2 m tidal amplitude, 33.75726° N, 118.41986° W) and inside (depth 10 ± 2 m tidal amplitude, 33.75712° N, 118.41842° W) the rocky substrate characterizing Marguerite Reef using 2 acoustic Doppler current profilers (ADCPs: 1200 kHz Workhorse Sentinel, Teledyne RD Instruments; see Fig. 1). ADCP deployments spanned the 2 experimental periods, from November 2016 through May 2018 and from April 2019 through September 2019. Prior to each deployment, the ADCPs underwent compass calibration and a series of sensor tests (WinSC Software; RD Instruments 2001). The ADCPs were mounted looking upward within a custom-made fiberglass frame which was positioned in a flat area on top of the benthos to minimize tilt of the sensors (Gaylord et al. 2007). The outside and inside ADCPs recorded 48 and 50 pings, respectively, per 3 min ensemble within 0.5 m vertical bins throughout the water column. The only exception to this protocol was that measurements collected in 2019 utilized a vertical bin size of 1 m. WinSC software was used to conduct an initial assessment of beam correlation, pitch, and roll for each deployment, and subsequent analyses were conducted using R v.4.0.2 (R Core Team 2021).

Raw velocity data were rotated to orient the horizontal Cartesian coordinates parallel (alongshore, u) and perpendicular (cross-shore, v) to the coast, with positive values of u upcoast and negative values of u downcoast. The emphasis in this study was on alongshore currents due to previous recognition of the former's greater degree of attenuation by kelp (Jackson 1998, Gaylord et al. 2007, Rosman et al. 2007). Velocity values in near-surface bins in the upper 10% of the water column were discarded due to data degradation associated with known side-lobe artefacts characteristic of acoustic profiles (Gunawan & Neary 2011). Velocity records from the remaining 90% of the water column were then averaged over 30 min blocks (Gunawan & Neary 2011).

2.4. Influence of kelp on depth-averaged currents

To examine *M. pyrifera*'s effect on the alongshore current velocities, 30 min averaged alongshore velocity data were depth-averaged and then partitioned into paired blocks of 10 d duration, one outside and one inside the reef habitat, each straddling a given kelp survey date. For each pair of 10 d time series, depth-averaged velocities outside of the reef were then regressed against those within the reef using major axis (MA) regression. This approach provided a quantitative assessment of the fractional decline in current speed on the reef in comparison to the simultaneous current speed outside of the reef habitat. A 1:1 slope would indicate no reduction in current speed on average when comparing the reef station to the station outside, while a smaller regression slope would indicate greater reduction of within-kelp current speeds compared to those outside. The slopes were then plotted as a function of stipe density to quantify the relationship between forest properties and the extent of current velocity damping. Note that because the topography and bathymetry between the 2 sensor locations remained

static throughout the study, the regression slopes corresponding to the zero-stipe case serve as reference points from which to compare further modifications due to kelp. Slopes were converted to a percentage of velocity reduction using:

$$P_i = (1 - slope_i) \cdot 100 \quad (1)$$

where P_i is the percentage of velocity reduced within the inner region of the reef, *slope* is the slope of the MA regression of velocities outside versus inside the reef, and i is the stipe density (unique for each kelp survey date). Percentages of velocity reduction were then compared across stipe densities, which varied through time, to determine the relationship between kelp forest structure and reductions in depth-averaged current speeds. A Šidák correction was applied to account for conducting multiple comparisons across the respective slopes. All statistical tests were accomplished in R v.4.0.2 (R Core Team 2021), with regressions and pairwise comparisons conducted using the package 'SMATR' (Warton et al. 2012).

2.5. Influence of subsurface canopy on alongshore currents

To quantify alongshore velocity reductions as the subsurface canopy emerged and extended up to the surface, MA regression slopes were computed using 30 min averaged alongshore velocity data from the 0.5 m vertical bin corresponding to the 25th, 50th, and upper 75th percentile of the water column relative to the bottom in addition to depth-averaged velocity data. Because the previous 10 d time series could obscure important patterns at shorter time scales relevant to subsurface canopy development, alongshore velocity data were re-partitioned into pairs of mini time series, one outside and one inside the reef, each spanning a 3 d period within each week for the dates ranging between 20 April 2017 and 14 July 2017. For each weekly 3 d time series, velocities outside of the reef were then regressed against those within the reef using MA regression to produce a slope for each of the 3 percentiles of the water column (25th, 50th, and 75th). Slopes were compared through time and for each water column percentile to determine the timing and degree of attenuation with respect to the subsurface canopy. Pairwise comparisons of the respective slopes were conducted using a Šidák correction. All statistical tests were accomplished in R v.4.0.2 (R Core Team 2021), with MA regressions and pairwise comparisons conducted using the package 'SMATR' (Warton et al. 2012).

3. RESULTS

3.1. Kelp forest dynamics

The structure of the *Macrocystis pyrifera* forest at Marguerite Reef varied considerably throughout this study. In late 2016 and into early 2017, the reef was devoid of vegetation (2016 data with zeros not shown). Following urchin culling in late 2016, new *M. pyrifera* recruits began to appear on the benthic substrate in mid-April 2017 and grew rapidly, reaching the water's surface in late June 2017 (Fig. 2A). Kelp canopy was first detected by satellite image analysis in July 2017, which was in accordance with diver observations. The percentage of maximum canopy cover averaged (±SE) 51.3 ± 3.9% between July 2017 and February 2018, after which the canopy roughly doubled its coverage, averaging 90.1 ± 0.68%. The site reached a maximum of 92% canopy cover in April 2018 (Fig. 2A). The kelp forest disappeared entirely in late 2018, resulting in the reef being once again devoid of vegetation. Canopy cover was detected next by satellite image analysis in June 2019, which was in accordance with diver observations. The percentage of canopy cover increased from 14.4% in June 2019 to 34.6% in November 2019, with an average of 26.8 ± 3.7% coverage over that timeframe (Fig. 2A).

Though not characterized in detail, continuous kelp canopy was also present upcoast and downcoast of the focal survey area. At the time of peak canopy coverage at our field site in April 2018 (Fig. 2A), the total distance of continuous kelp canopy extended 1800 m in the alongshore direction. The distance from the inside ADCP to the upcoast boundary of the forest was 1450 m long, while the distance from the inside ADCP to the downcoast boundary of the forest was 350 m long.

Stipe density increased sharply from 0 stipes m^{-2} in mid-April 2017 to 6.2 ± 1.9 stipes m^{-2} in late June 2017, reaching a maximum of 7.9 ± 1.5 stipes m^{-2} in late July 2017 (Fig. 2B). The forest subsequently underwent a period of thinning, as indicated by a reduction in both stipe density and kelp density (ind. m^{-2}) from October 2017 into May 2018 (Fig. 2B,C). While stipe and kelp densities slowly decreased beginning in October 2017, the size of remaining kelp individuals continued to increase into early spring 2018, as indicated by a gradual increase in kelp size (i.e. stipes ind.$^{-1}$), from 2 ± 0.2 stipes ind.$^{-1}$ in May 2017 to a maximum of 7.6 ± 0.8 stipes ind.$^{-1}$ in May 2018 (Fig. 2D). Such a pattern indicates a shift in the

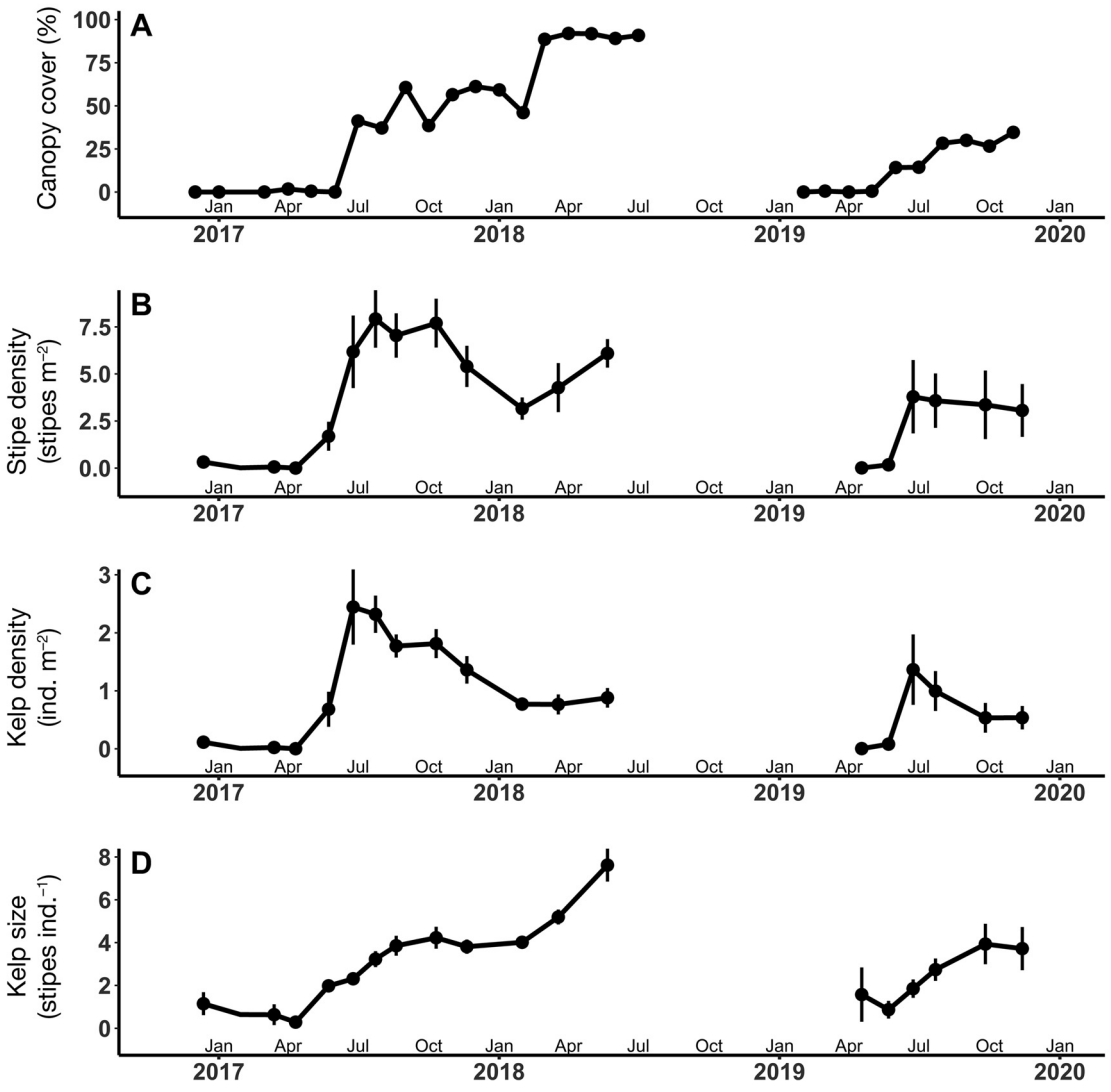

Fig. 2. Changes in the *Macrocystis pyrifera* kelp forest structure at Marguerite Reef over the duration of the study: (A) percentage of canopy cover at the surface, (B) stipe density, (C) kelp density, and (D) stipes per kelp individual. Points: mean across transects; vertical bars: ±SE. Canopy coverage is the percent of kelp coverage over a rectangular area (see Fig. 1), overlapping with the subtidal kelp surveys (n = 8)

structural composition of the forest; i.e. a shift from a forest composed of many plants each supporting a handful of stipes to one composed of fewer but larger individuals. In December 2018, Marguerite Reef experienced a complete loss of its subtidal vegetation.

In June of 2019, Marguerite Reef again transitioned from a reef composed of bare rock to one supporting a forest with surface canopy. Stipe density increased from 0 stipes m^{-2} in April 2019 to 3.8 ± 2.0 stipes m^{-2} in June 2019 and averaged 3.4 ± 0.2 stipes m^{-2} between June and October 2019. Densities of kelp individuals initially increased to 1.4 ± 0.6 ind. m^{-2} in June 2019, and then subsequently decreased to 0.5 ± 0.3 ind. m^{-2} by October 2019. The size of the kelp individuals gradually increased throughout forest development, reaching a maximum of 4 ± 0.9 stipes ind.$^{-1}$ by October 2019. While general forest growth patterns were similar between the 2 experimental periods (2017 and 2019), when compared over the same timeframe following initial forest growth (i.e. May through November), the magnitude of peak plant and stipe densities as well as canopy coverage in 2019 were approximately ⅓ to ½ of those observed in the 2017 experiment.

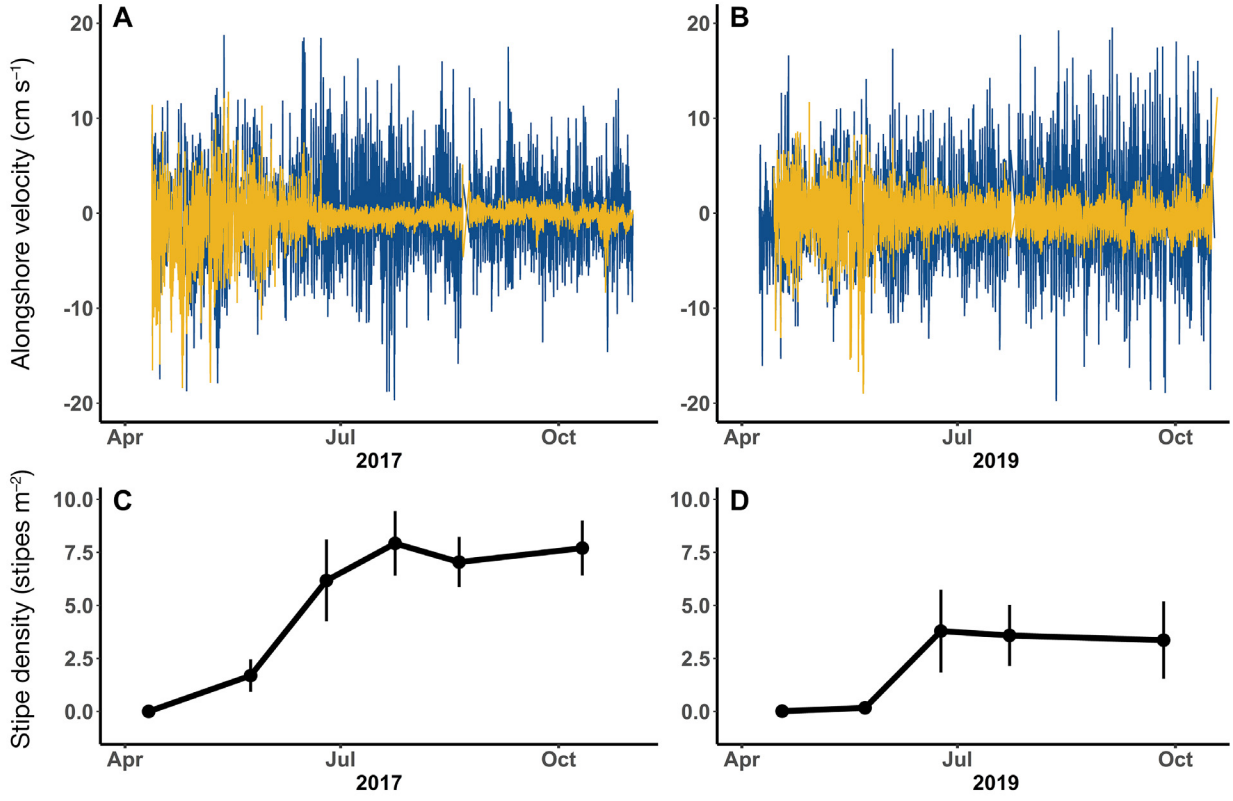

Fig. 3. Depth-averaged alongshore velocities outside (blue lines) and inside (yellow lines) Marguerite Reef as a new kelp forest emerged between April and October in (A) 2017 and (B) 2019. Mean (±SE) *Macrocystis pyrifera* stipe densities at Marguerite Reef between April and October (C) 2017 and (D) 2019

3.2. Influence of kelp on depth-averaged alongshore currents

Alongshore current velocities above the reef were lower than those outside of the reef habitat in the absence of kelp (stipe density < 0.2 stipes m^{-2}), consistent with the tendency for alongshore currents to be slower in shallower water due to shoreline boundary layer effects (Nickols et al. 2012, 2015). Currents in the reef habitat were then further reduced once the kelp forest developed. Kelp had a striking effect on alongshore current velocities within the reef habitat, as readily seen by the decrease in velocities observed at the inner sensor station (Fig. 3, represented in yellow), which contrasts with the roughly unchanging pattern of velocities at the sensor station outside of the reef (Fig. 3, represented in blue). Sharp reductions in alongshore velocities within the inner region of the reef habitat coincided with an increase in kelp stipe densities in both 2017 and 2019. In contrast, alongshore velocities remained high and variable outside of the reef habitat. Slow alongshore velocities persisted above the reef throughout the summer months and into the fall of each year, highlighted by the slower and less variable velocities observed at the inner sensor station in contrast to the faster and more variable velocities observed at the outer sensor station (Fig. 3).

Comparison of root mean square (rms) velocities outside and within the reef habitat throughout forest development provides a general quantitative metric for characterizing the influence of kelp on average alongshore current speeds (Table 1). For example, alongshore rms velocities at the inner sensor station remained slow (i.e. less than 1 cm s^{-1}) throughout the summer and into fall 2017, while rms velocities outside the reef habitat fluctuated between 3.2–4.9 cm s^{-1} (Table 1). Similarly, throughout the summer and into fall 2019, alongshore rms velocities inside the reef habitat remained less than 1.5 cm s^{-1}, while rms velocities outside the reef habitat ranged between 3.7–6.1 cm s^{-1} (Table 1).

While informative, comparisons of rms velocities do not fully capture the underlying physical relationship between the 2 sensor stations. Comparing MA regression slopes of velocities outside and

Table 1. Summary statistics for depth-averaged alongshore velocities (cm s^{-1}) outside and inside the reef. Summary statistics were computed over a duration of 10 d, spanning a total of 20 tidal cycles each. Summary statistics include root mean square (rms) velocity outside and inside Marguerite Reef. Each of the 10 d velocity timeseries (also represented in Fig. 4) corresponds to a unique subtidal kelp survey date

Experiment	Kelp survey date (yyyy-mm-dd)	Stipe density (m^{-2})	Depth-averaged alongshore rms velocity (cm s^{-1})	
			Outside	Inside
2017	2017-01-29	0.014	4.167	2.693
2017	2017-04-11	0.002	3.916	3.761
2017	2017-05-24	1.692	4.340	3.024
2017	2017-06-25	6.173	4.893	0.817
2017	2017-07-24	7.919	4.008	0.640
2017	2017-08-20	7.042	4.670	0.684
2017	2017-10-11	7.698	3.195	0.766
2017	2017-11-20	6.092	3.408	0.786
2017	2018-01-31	3.160	3.443	0.834
2017	2018-03-19	4.271	4.101	1.422
2017	2018-05-22	6.092	3.383	1.555
2019	2019-04-18	0.013	4.705	3.281
2019	2019-05-23	0.173	4.346	3.359
2019	2019-06-24	3.788	3.665	1.067
2019	2019-07-23	3.581	4.858	1.241
2019	2019-09-26	3.360	6.130	1.420
2019	2019-11-13	3.060	5.521	1.310

within the reef provides a more direct metric by which to calculate percent velocity reduction due to the presence of kelp (Fig. 4). Velocity reductions that occur in the absence of kelp can be attributed to frictional losses due to interactions with the benthos and differences in sensor station depths within the coastal boundary layer (Nickols et al. 2012). Further velocity reductions can be attributed to the presence of kelp at a given stipe density (or forest structure).

A sudden change in velocity reductions occurred at a threshold forest structure of 3 stipes m^{-2}, at which much of the depth-averaged velocity reduction occurred (Fig. 4). In the absence of kelp (stipe densities ≤ 0.173), regression slopes ranged from 0.46–0.85, representative of current reductions associated with seafloor friction and broader coastal boundary layer effects. In contrast, once the forest reached 3 stipes m^{-2} and the canopy was at the surface, slope regressions dropped uniformly to values below 0.12, indicating that velocities within the reef habitat were 12% of those outside of the reef habitat. Further reductions in depth-averaged velocities also arose with increasing stipe density (Fig. 5). Interestingly, when stipe densities were low (i.e. 1.7 stipes m^{-2}) and the forest canopy had not yet reached the surface, depth-averaged velocity reductions were not detectably different from the no-kelp regressions.

3.3. Influence of subsurface canopy on alongshore currents

While depth-averaged velocity reductions were detectable only after a surface canopy began to form, reduced velocities were readily visible in the lower region of the velocity profile beforehand (Fig. 6). A subsurface canopy 'shadow' characterized by reduced velocities was apparent within the inner region of the reef habitat and rapidly changed in height as the canopy grew toward the surface.

Distinct regions of the water column exhibited temporal lags in the extent of velocity reduction as the subsurface canopy developed. Initial observations of single-bladed kelp recruits blanketing the benthos occurred in mid-April 2017. Alongshore velocities in the 25th percentile of the water column (near-bottom) were reduced by >99% by 57 d post-recruitment (Fig. 7). Conditions of near-100% velocity reduction in the 50th (middle) and 75th (near-surface) percentiles took an additional 14 and 21 d, respectively.

4. DISCUSSION

In this study, we quantified reductions in alongshore current velocities across successional stages of a restored *Macrocystis pyrifera* forest at Marguerite Reef, Palos Verdes, California. Over the course of the study, the reef twice underwent a transition from a barren state, devoid of vegetation, to one in which a kelp forest was present. Peak forest densities in both the 2017 and 2019 experiments were within typical ranges of mature *M. pyrifera* forests in California (1.9–15 stipes m^{-2} and up to 3 plants m^{-2}; North 1971). Depth-averaged alongshore velocities above the reef decreased abruptly upon initial formation of the surface canopy and stipe density reaching roughly 3 stipes m^{-2}. Stipe density exhibited a positive relationship with depth-averaged velocity attenuation. Velocity attenuation in the upper region of the water col-

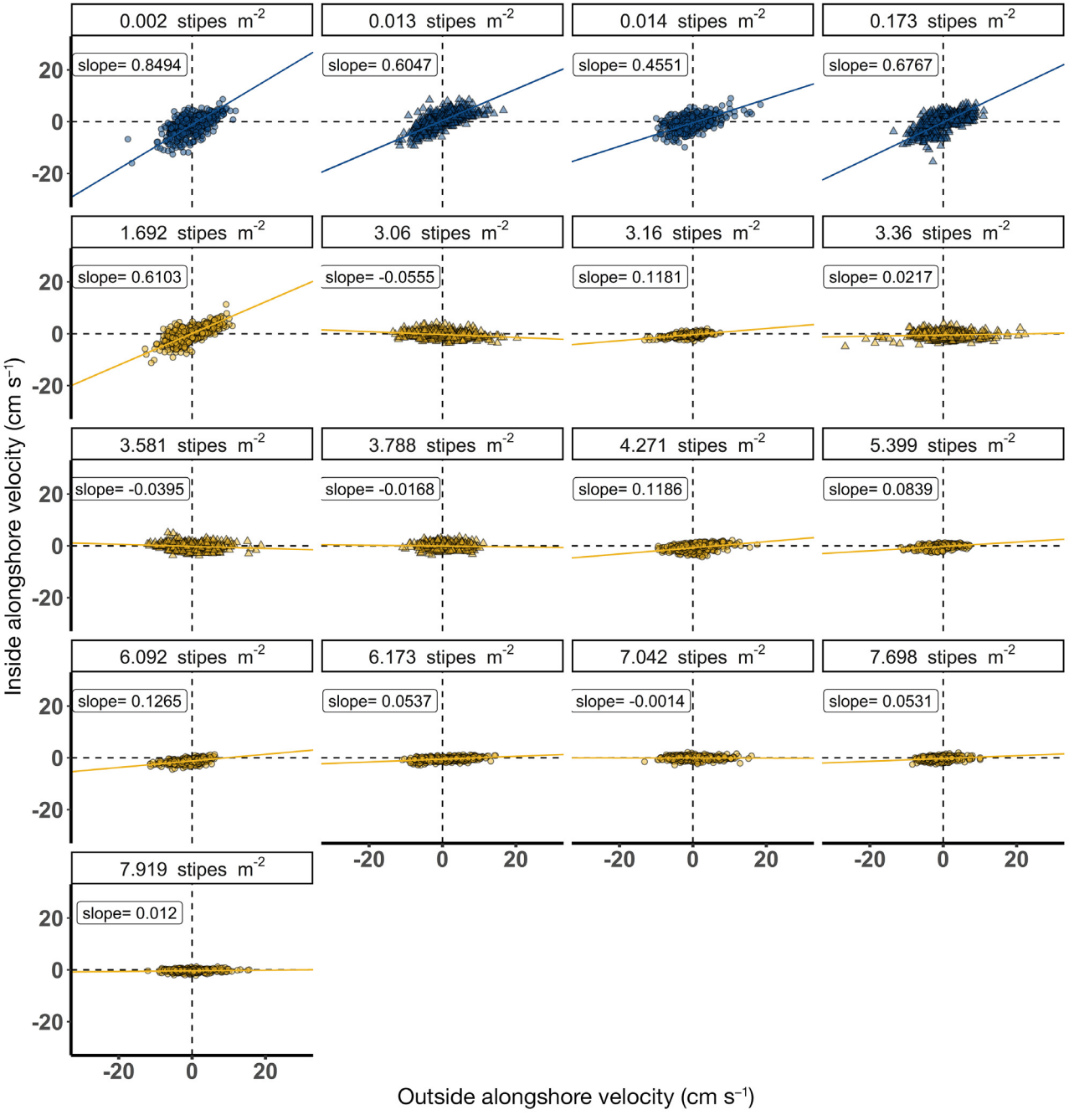

Fig. 4. Major axis regressions of depth-averaged alongshore velocities outside and inside Marguerite Reef, across stipe densities. Plots are ordered and labeled by stipe density; corresponding survey dates can be found in Table 1. Lines: major axis regression slope; points: depth-averaged velocities corresponding with a given survey date. Blue coloration: relationships when negligible kelp was present (stipe density < 0.2); golden-brown coloration: relationships when kelp was present (stipe density > 0.2). Circles: data from the 2017 experiment; triangles: 2019

umn lagged behind that of the lower region of the water column by a little over 1 mo, revealing a seasonally changing velocity profile that could have important implications for community residents and for kelp itself.

4.1. Forest structure

Stipe density governs much of the attenuation of alongshore current velocity observed at Marguerite Reef, but there are likely additional drivers at play.

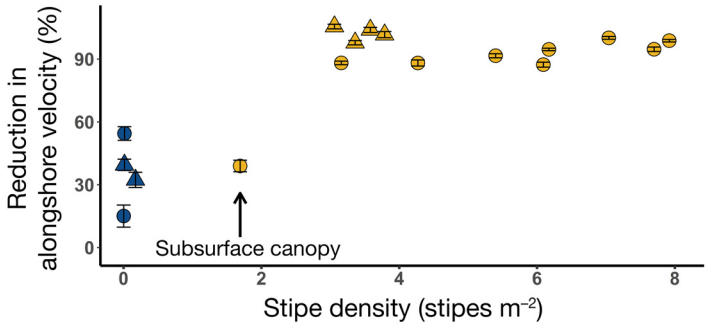

Fig. 5. Reduction in alongshore velocities within Marguerite Reef across stipe densities. Points: percent velocity reductions (computed from major axis regression slopes) associated with each stipe density; vertical bars: ±SE; blue points: no kelp present (stipe density < 0.2); yellow points: kelp present (stipe density > 0.2); circles: data from the 2017 experiment; triangles: 2019. Arrow labeled 'subsurface canopy' indicates when kelp was present but not yet at the surface

Forest age and size of the kelp plants are also important. For example, Marguerite Reef exhibited a lesser degree of velocity reduction when the kelp forest was 'older' and composed of fewer but larger individuals for a given stipe density (Figs. 2 & S1 in the Supplement at www.int-res.com/articles/suppl/m694p045_supp.pdf). These data suggest that 2 forests supporting the same stipe density but different 'ages' likely would not exhibit the same degree of alongshore current attenuation — all else being equal, the 'younger' forest would likely exhibit a greater degree of attenuation (Fig. S1). Therefore, the level of forest maturation may be a largely overlooked driver of alongshore current damping potential.

Additionally, although the presence of a surface canopy appeared to be critical to the detection of kelp-associated reductions in depth-averaged velocity, additional canopy cover did not correspond with increased velocity reductions. Consequently, canopy cover per se may not be a dominant determinant of the degree of current attenuation, as discussed in previous studies (Rosman et al. 2007), and perhaps is a less useful metric for predicting current attenuation of mature forests at finer temporal scales (e.g. intra-annual). Stipe density, kelp density, kelp size, and

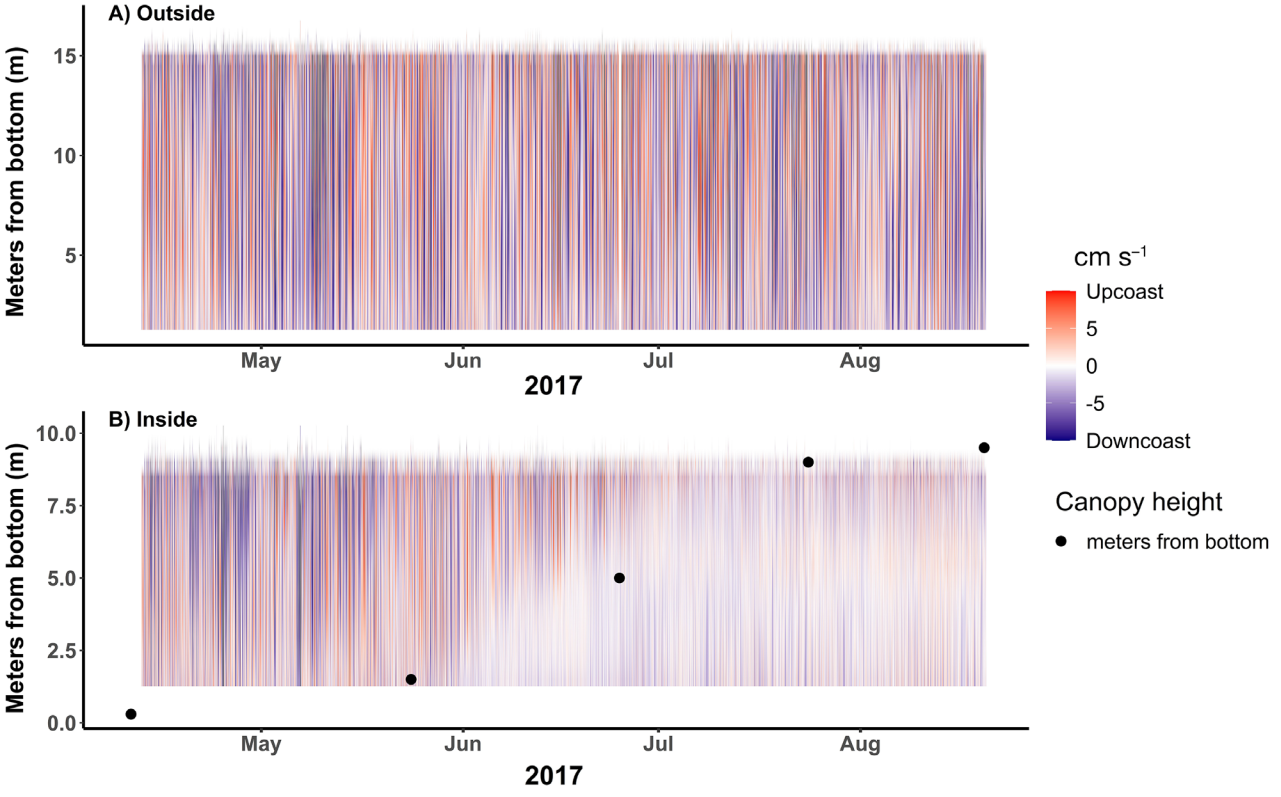

Fig. 6. Time series of alongshore velocity profiles (A) outside and (B) inside Marguerite Reef, spanning the transition from a barren reef to one supporting a kelp forest with a surface canopy. Red: upcoast flows; blue: downcoast flows. Darker shades: greater velocities; lighter shades: slower velocities; white: 0 cm s^{-1}. Black points in (B) represent kelp canopy heights estimated by divers during each kelp survey. The April timepoint corresponds to the first sighting of single-bladed kelp recruits on the benthos; it appears below the shaded portion of the graph because velocity data are available only down to within ~2 m of the seafloor due to the finite size and sensing limitations of the recording instrument

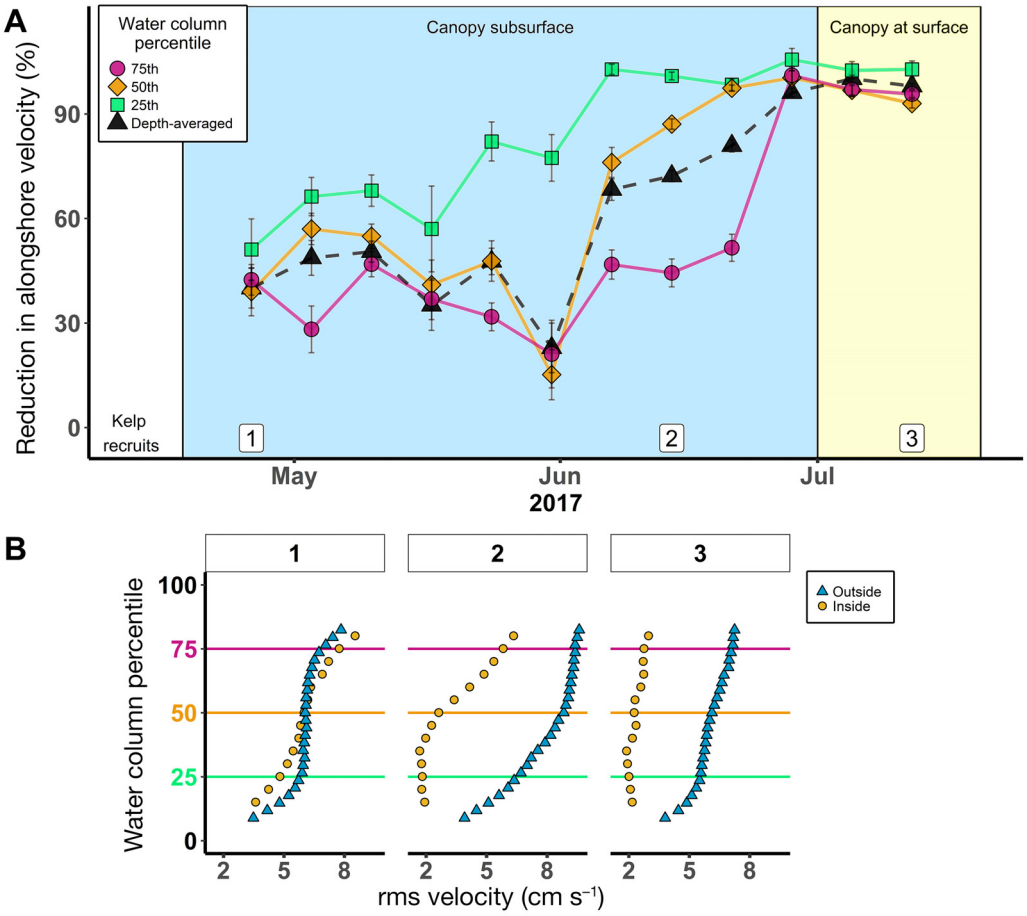

Fig. 7. Extent of alongshore velocity reduction within the Marguerite Reef kelp forest habitat in 2017 varies throughout the water column as a subsurface canopy emerges and grows to the surface. (A) Percent velocity reductions of weekly averaged flow speeds. Vertical bars: ±SE. Black triangles represent depth-averaged data, and green squares, orange diamonds, and pink circles represent data from velocities at the 25th, 50th and 75th percentile positions of the water column, respectively. White region: period when single-bladed kelp recruits were first observed; blue region: when kelp fronds (stipes plus blades) remained subsurface; yellow region: when a surface canopy was present. (B) Average root mean square (rms) velocity quantified at multiple heights throughout the water column to provide a depth-specific vertical profile of horizontal velocity, corresponding to box numbers 1–3 in (A). Blue and yellow points: values from outside and inside the reef habitat, respectively. Horizontal lines: positions in the water column that correspond to the time series in (A)

canopy cover measured in this study covaried, however, limiting our capacity to quantitatively determine the effects of differing forest structures on the degree of velocity reduction. All of these factors, therefore, warrant future investigation. Additionally, while changes in kelp canopy cover likely impact surface flows, bottom-mounted, upward-looking ADCPs are unable to reliably characterize surface current velocities (Gunawan et al. 2011), necessitating an alternative experimental approach in future work to understand drivers of attenuation of surface currents.

Alongshore velocity attenuation can depend on kelp plant density and alongshore distance traveled into the forest (Gaylord et al. 2012). This same effect has been documented in seagrass meadows and other aquatic vegetation (Colomer et al. 2017, Layton et al. 2019). Therefore, the precise levels of velocity reduction documented in this study and others may depend on the exact location of the instruments relative to the leading edges of the forest. For example, in April 2018, the alongshore extent of continuous canopy was asymmetrical with respect to the position of the inside ADCP, such that canopy distance upcoast was over 4 times the distance downcoast. One might expect a greater degree of attenuation in downcoast currents, after transiting through a greater distance of kelp, than upcoast currents, which transited through a lesser distance of kelp. Interestingly, however, we did not observe strong differences in upcoast and downcoast velocity reduction around this time period

(Fig. 4), suggesting limited effects of asymmetry in neighboring kelp extent. Edge effects, and consequently forest size, may play less of a role in driving the degree of alongshore attenuation once the alongshore distance traveled reaches an upper threshold. Potential roles of neighboring kelp forests, degree of continuity/patchiness, and the sizes at which they become important warrant future exploration.

4.2. Subsurface canopy

Depth-specific velocity reductions above the reef align temporally and spatially with anticipated changes in subsurface canopy height. In late May 2017, velocity reductions detected at the bottom 25th percentile position of the water column coincided with an increase in velocities in the middle of the water column, as represented by a decrease followed by an abrupt reduction in the middle 50th percentile position in Fig. 7. As alongshore velocities encounter an obstacle, in this case a subsurface canopy, the water must either re-route laterally around the obstacle or vertically above the obstacle. While water is likely also re-routed laterally, the spike in velocities in the region above the subsurface canopy, observed in late May 2017 at the middle 50th percentile position of the water column and to a lesser degree in late June 2017 at the upper 75th percentile position of the water column, suggests water is being re-routed vertically, producing faster velocities just above the subsurface canopy. Submerged canopies formed by seagrasses and macroalgae can also significantly alter the shape of the current velocity profile (Andersen et al. 1996, Løvås & Tørum 2001, Bryan et al. 2007, Abdolahpour et al. 2017, Kregting et al. 2021). In the case of an established forest supporting a surface canopy, vertical re-routing is physically constrained by the sea surface, and thus water is redirected around the lateral edges of the forest, manifesting as accelerated velocities along the forest edges as observed in previously studied *M. pyrifera* forests (Jackson & Winant 1983, Jackson 1998, Gaylord et al. 2007).

Relevance of the physical process of re-routed water is not limited to emerging kelp forests. Established and multi-year-old giant kelp forests, such as those commonly found in Southern California, experience a seasonal surge of new recruits in springtime. Data shown in Figs. 6 & 7 suggest that roughly annual pulses of new kelp recruits could further modify the profile of alongshore velocity reductions. This trend could be of particular importance to not only the kelp itself, via altered nutrient transport, but to the myriad community members that occupy the kelp forest. For example, many benthic invertebrates are broadcast spawners and rely on water motion to facilitate fertilization of eggs and sperm (Crimaldi & Zimmer 2014) as well as transport of their larvae across multiple temporal and spatial scales (Pineda et al. 2007). Importantly, alterations of the spatial patterns of current velocities can have consequences for the fate of both local dispersers with short larval durations (i.e. minutes to days), such as the colonial tunicate *Tridemnum solidum* (Shanks 2009), and longer distance dispersers with long larval durations (i.e. weeks to months), such as the purple urchin *Strongylocentrotus purpuratus* (Heyland & Hodin 2014). Furthermore, while benthic suspension feeders rely on water motion to deliver phytoplankton and other suspended food sources to near-bed regions of the water column where they live (Pequegnat 1964, Page et al. 2008), other planktivores, such as rockfish, rely on the delivery of zooplankton to regions higher in the water column, where adults and juveniles of some species reside (Pequegnat 1964, Gaines & Roughgarden 1987).

4.3. Residence time

Modifications to the alongshore current velocity profile can also have profound effects on the residence time of water, particularly in lower regions of the water column as cohorts of new kelp recruits emerge. Reduced current velocities, as observed in this study, can lengthen residence times of water internal to the kelp forest, which in turn can lead to increases in chemical stratification and nutrient depletion. For example, slower flows increase the amount of time kelp is in contact with a given pool of water, determining the capacity of kelp to chemically modify the water properties through photosynthetic uptake of CO_2 and production of oxygen (Hirsh et al. 2020, Traiger et al. 2022). Because much of the kelp-driven chemical alteration occurs in the surface waters where the photosynthetic biomass is concentrated, the water column can become chemically stratified, creating chemically distinct regions within the water column (Traiger et al. 2022). Severely reduced velocities, such as those observed following surface canopy formation in both the 2017 and 2019 experiments, can further exacerbate differences in water column chemistry. Additionally, entrapment of poorly oxygenated waters can occur within depressions of the rocky reef, creating 'internal tide pools,' which can be particularly consequential for kelp forest organisms residing in the lower region of the wa-

ter column (Leary et al. 2017). Residence time of low-oxygen water within these pools is likely increased in scenarios such as those observed throughout June 2017, when the emerging subsurface canopy attenuated much of the alongshore velocities in the lower region of the water column. Further, reductions in near-bottom current velocities can limit the influx and lateral transport of nutrient-replete waters throughout the forest (Fram et al. 2008), which can drive temporal and spatial patterns of forest recovery following restoration as well as forest growth more broadly (Stewart et al. 2009). Each of these biophysical and biochemical processes contribute to the patchy mosaic of water column properties experienced by kelp forest community members. Importantly, attenuation of flows occurs to varying degrees in different regions of the water column depending on forest growth and structure which, in turn, can exacerbate or ameliorate stressors, such as ocean acidification, hypoxia, or nutrient repletion.

4.4. Transport of particulates and detritus

Currents can interact with kelp to control sediment transport and suspension of particles within the water column, influencing patterns of kelp persistence and benthic community composition through processes such as benthic scour, reef burial, and reduced light penetration (Eckman et al. 1989, Shiel & Foster 2015, Watanabe et al. 2016, Tait 2019). While strong current velocities can result in sediments being transported long distances across reefs (Ferré et al. 2010), the presence of a kelp forest likely impedes alongshore sediment transport and facilitates localized sediment accretion through attenuation of currents. Reduced alongshore transport of sediments can be of particular concern for rocky reef communities found adjacent to coastal regions prone to erosion and landslides, such as the Palos Verdes Peninsula (Ferré et al. 2010). For example, sediment plumes following landslides can reduce species diversity and biomass as well as shift benthic community composition in adjacent impacted kelp forest communities (Kiest 1993). Beyond direct burial of existing benthic community members, increased sedimentation can limit recruitment of kelp and other benthic species by obstructing substrate attachment, scouring new individuals, or inhibiting light; the latter of which is particularly consequential for early life stages of primary producers (Watanabe et al. 2016, Tait 2019). Reduced light penetration caused by increased turbidity severely reduces kelp productivity (Blain et al. 2021) and drives the assemblage of macroalgal community structure and composition (Shepherd et al. 2009). Interestingly, such consequences of altered sediment transport and particle suspension likely contributed to the temporal patterns of kelp forest structure observed in this study. The complete loss of subtidal vegetation at Marguerite Reef in late 2018 coincided with a landslide that occurred just up the coast, with the winter of 2019 exhibiting higher turbidity levels than in the winter of 2018 (Rukstales et al. unpubl. data). Partial reef burial and increase in water column particulates resulted in a thin layer of sediment covering the blades that persisted at the site throughout the 2019 experiment. Subsequent forest recovery observed in the 2019 experiment was significantly less than what was observed in the 2017 experiment and was likely driven in part by biophysical feedbacks among kelp, alongshore currents, and sediment influx. While giant kelp forests have little capacity for coastal protection by way of attenuation of surface gravity waves (Elwany et al. 1995, Elsmore 2021), waves may contribute significantly to processes of sediment entrainment, resuspension, and deposition within the coastal zone. These and other wave effects, as well as their capacity to interact with currents that themselves are modified by the presence of kelp (Grant & Madsen 1986, Gaylord et al. 2002, 2004), are beyond the scope of this study, although a subset of these biophysical processes are explored in a companion work (Elsmore 2021).

5. CONCLUSIONS

This study quantified reductions in alongshore velocities within reef habitat that twice underwent a transition from a barren state to one supporting a kelp forest with a surface canopy. Reductions in depth-averaged velocities increased with increasing stipe density once a surface canopy was present. Subsurface canopy development resulted in temporal and spatial lags in current attenuation depending on vertical position in the water column. In particular, when the kelp was short, velocity was reduced in the lower part of the water column only. When kelp reached the surface, velocity was reduced over the full water column. Our results reinforce existing literature showing giant kelp forests have the capacity to substantially modify alongshore currents and provide new insights into the role forest structure plays in determining the degree of flow reduction and its spatial and temporal patterns. These findings have implications for larval, nutrient, detrital, and sediment transport in the nearshore environment.

Acknowledgements. This work was supported by the California State Coastal Conservancy (grant number 15-013), National Science Foundation (NSF) (grant number OCE-1636191), University of Southern California, Sea Grant (grant number NA180AR4170075), and Dolby Laboratories. K.E. was additionally supported by an NSF Graduate Research Fellowship, Bilinski Fellowship, and a Norcal Society of Environmental Toxicology and Chemistry grant. The authors are grateful to A. Barilotti, H. Burdick, B. Cohn, C. Dibble, K. Dubois, G. Elsmore, B. Grimes, T. Herzik, J. Hollarsmith, P. House, A. Ninokawa, D. Panos, A. Saley, A. Sparks, B. Sterling, G. Thompson, A. Ullmann, and M. Ward for field and logistical assistance.

LITERATURE CITED

Abdolahpour M, Hambleton M, Ghisalberti M (2017) The wave-driven current in coastal canopies. J Geophys Res Oceans 122:3660–3674

Andersen KH, Mork M, Nilsen JEO (1996) Measurements of the velocity-profile in and above a forest of *Laminaria hyperborea.* Sarsia 81:193–196

Blain CO, Hansen SC, Shears NT (2021) Coastal darkening substantially limits the contribution of kelp to coastal carbon cycles. Glob Change Biol 27:5547–5563

Bryan KR, Tay HW, Pilditch CA, Lundquist CJ, Hunt HL (2007) The effects of seagrass (*Zostera muelleri*) on boundary-layer hydrodynamics in Whangapoua Estuary, New Zealand. J Coast Res Spec Issue 50:668–672

Burdick H, Ford T, Reynolds A, House P and others (2016) Palos Verdes kelp forest restoration project, year 3: July 2015–June 2016. The Bay Foundation, Los Angeles, CA

Cavanaugh KC, Siegel DA, Reed DC, Dennison PE (2011) Environmental controls of giant-kelp biomass in the Santa Barbara Channel, California. Mar Ecol Prog Ser 429:1–17

Colomer J, Soler M, Casamitjana X, Oldham C (2017) Impact of anthropogenically created canopy gaps on wave attenuation in a *Posidonia oceanica* seagrass meadow. Mar Ecol Prog Ser 569:103–116

Crimaldi JP, Zimmer RK (2014) The physics of broadcast spawning in benthic invertebrates. Annu Rev Mar Sci 6: 141–165

Dayton PK, Currie V, Gerrodette T, Keller BD, Rosenthal R, Tresca DV (1984) Patch dynamics and stability of some California kelp communities. Ecol Monogr 54:253–289

Eckman JE, Duggins DO, Sewell AT (1989) Ecology of understory kelp environments. I. Effects of kelps on flow and particle transport near the bottom. J Exp Mar Biol Ecol 129:173–187

Elsmore KE (2021) Consequences of kelp loss: using restoration as a tool to inform ecology. PhD dissertation, University of California, Davis, CA

Elwany MHS, O'Reilly WC, Guza RT, Flick RE (1995) Effects of Southern California kelp beds on waves. J Waterw Port Coast Ocean Eng 121:143–150

Ferré B, Sherwood AR, Wiberg PL (2010) Sediment transport on the Palos Verdes shelf, California. Cont Shelf Res 30:761–780

Fram JP, Stewart HL, Brzezinski MA, Gaylord B, Reed DC, Williams SL, MacIntyre S (2008) Physical pathways and utilization of nitrate supply to the giant kelp, *Macrocystis pyrifera.* Limnol Oceanogr 53:1589–1603

Frieder CA, Nam SH, Martz TR, Levin LA (2012) High temporal and spatial variability of dissolved oxygen and pH in a nearshore California kelp forest. Biogeosciences 9: 3917–3930

Gaines SD, Roughgarden J (1987) Fish in offshore kelp forests affect recruitment to intertidal barnacle populations. Science 235:479–481

Gaylord B, Gaines SD (2000) Temperature or transport? Range limits in marine species mediated solely by flow. Am Nat 155:769–789

Gaylord B, Reed DC, Raimondi PT, Washburn L, McLean SR (2002) A physically based model of macroalgal spore dispersal in the wave and current-dominated nearshore. Ecology 83:1239–1251

Gaylord B, Reed DC, Washburn L, Raimondi PT (2004) Physical–biological coupling in spore dispersal of kelp forest macroalgae. J Mar Syst 49:19–39

Gaylord B, Reed DC, Raimondi PT, Washburn L (2006) Macroalgal spore dispersal in coastal environments: mechanistic insights revealed by theory and experiment. Ecol Monogr 76:481–502

Gaylord B, Rosman JH, Reed DC, Koseff JR and others (2007) Spatial patterns of flow and their modification within and around a giant kelp forest. Limnol Oceanogr 52:1838–1852

Gaylord B, Nickols KJ, Jurgens L (2012) Roles of transport and mixing processes in kelp forest ecology. J Exp Biol 215:997–1007

Graham MH, Vasquez JA, Buschmann AH (2007) Global ecology of the giant kelp Macrocystis: from ecotypes to ecosystems. Oceanogr Mar Biol Annu Rev 45:39–88

Grant WD, Madsen OS (1986) Combined wave and current interaction with a rough bottom. Annu Rev Fluid Mech 18:265–305

Grime B, Sanders R, Burdick H, Ford T, Williams J, Williams C, Pondella D (2020) Palos Verdes kelp forest restoration project, year 7: July 2019–June 2020. The Bay Foundation, Los Angeles, CA

Gunawan B, Neary VS (2011) ORNL ADCP post-processing guide and MATLAB algorithms for MHK site flow and turbulence analysis. Report No. ORLN/TM-2011/404. Oak Ridge National Laboratory, Oak Ridge, TN

Heyland A, Hodin J (2014) A detailed staging scheme for late larval development in *Strongylocentrotus purpuratus* focused on readily-visible juvenile structures within the rudiment. BMC Dev Biol 14:22

Hirsh HK, Nickols KJ, Takeshita Y, Traiger SB, Mucciarone DA, Monosmith S, Dunbar RB (2020) Drivers of biogeochemical variability in a Central California kelp forest: implications for local amelioration of ocean acidification. J Geophys Res 125:e2020JC016320

Hurd CL (2000) Water motion, marine macroalgal physiology, and production. J Phycol 36:453–472

Jackson GA (1998) Currents in the high drag environment of a coastal kelp stand off California. Cont Shelf Res 17: 1913–1928

Jackson GA, Winant CD (1983) Effect of a kelp forest on coastal currents. Cont Shelf Res 2:75–80

Kiest K (1993) The influence of sediment from landslide plumes on sessile kelp forest assemblages. MS thesis, San Jose State University, San Jose, CA

Konotchick R, Parnell PE, Dayton PK, Leichter JJ (2012) Vertical distribution of *Macrocystis pyrifera* nutrient exposure in southern California. Estuar Coast Shelf Sci 106: 85–92

Koweek DA, Nickols KJ, Leary PR, Litvin SY and others (2017) A year in the life of a central California kelp forest:

physical and biological insights into biogeochemical variability. Biogeosciences 14:31–44
Kregting LT, Stevens CL, Cornelisen CD, Pilditch CA, Hurd CL (2011) Effects of small-bladed macroalgal canopy on benthic boundary layer dynamics: implications for nutrient transport. Aquat Biol 14:41–56
Kregting L, Britton D, Mundy CN, Hurd C (2021) Safe in my garden: reduction of mainstream flow and turbulence by macroalgal assemblages and implications for refugia of calcifying organisms from ocean acidification. Front Mar Sci 8:693695
Layton C, Shelamoff V, Cameron MJ, Tatsumi M, Wright JT, Johnson CR (2019) Resilience and stability of kelp forests: the importance of patch dynamics and environment–engineer feedbacks. PLOS ONE 14:e0210220
Leary PR, Woodson CB, Squibb ME, Denny MW, Monosmith SG, Micheli F (2017) 'Internal tide pools' prolong kelp forest hypoxic events. Limnol Oceanogr 62:2864–2878
Løvås SM, Tørum A (2001) Effect of the kelp *Laminaria hyperborea* upon sand dune erosion and water particle velocities. Coast Eng 44:37–63
McPhee-Shaw EE, Siegel DA, Washburn L, Brzeeinski MA, Jones JL, Leydecker A, Melak J (2007) Mechanisms for nutrient delivery to the inner shelf: observations from the Santa Barbara Channel. Limnol Oceanogr 52:1748–1766
Morgan SG, Miller SH, Robart MJ, Largier JL (2018) Nearshore larval retention and cross-shelf migration of benthic crustaceans at an upwelling center. Front Mar Sci 5:161
Nickols KJ, Gaylord B, Largier JL (2012) The coastal boundary layer: predictable current structure decreases alongshore transport and alters scales of dispersal. Mar Ecol Prog Ser 464:17–35
Nickols KJ, White JW, Largier JL, Gaylord B (2015) Marine population connectivity: reconciling large-scale dispersal and high self-retention. Am Nat 185:196–211
Noble MA, Rosenberger KJ, Hamilton P, Xu JP (2009) Coastal ocean transport patterns in the central Southern California Bight. In: Lee HJ, Normark WR (eds) Earth science in the urban ocean: the Southern California continental borderland. Special Paper No. 454. The Geological Society of America, Boulder, CO, p 193–226
North WJ (1971) The biology of giant kelp beds (*Macrocystis*) in California. Nova Hedwigia 32:1–600
Page HM, Reed DC, Brzezinski MA, Melack JM, Dugan JE (2008) Assessing the importance of land and marine sources of organic matter to kelp forest food webs. Mar Ecol Prog Ser 360:47–62
Panos DA (2022) Biogeochemical variability of temperate rocky reefs: physical conditions determine detection of biological signals. MS thesis, California State University, Northridge, CA. http://hdl.handle.net/10211.3/222071
Pequegnat WE (1964) The epifauna of a California siltstone reef. Ecology 45:272–283
Pineda J, Hare JA, Sponaugle S (2007) Larval transport and dispersal in the coastal ocean and consequences for population connectivity. Oceanography (Wash DC) 20:22–39
Planet (2021) Planet imagery product specifications. https://assets.planet.com/docs/Planet_Combined_Imagery_Product_Specs_letter_screen.pdf
R Core Team (2021) R: a language and environment for statistical computing. R Foundation for Statistical Computing, Vienna
Raimondi PT, Reed DC, Gaylord B, Washburn L (2004) Effects of self-fertilization in the giant kelp, *Macrocystis pyrifera*. Ecology 85:3267–3276
RD Instruments (2001) WorkHorse sentinel ADCP user's guide. https://epic.awi.de/id/eprint/40219/1/ADCP_Sentinel_User_Guide.pdf
Reed DC, Kinlan BP, Raimondi PT, Washburn L, Gaylord B, Drake PT (2006) A metapopulation perspective on the patch dynamics of giant kelp in Southern California. In: Kritzer J, Sale P (eds) Marine metapopulations. Academic Press, San Diego, CA, p 352–386
Reed D, Rassweiler A, Arkema K (2009) Density derived estimates of standing crop and net primary production in the giant kelp *Macrocystis pyrifera*. Mar Biol 156:2077–2083
Rodriguez GE, Rassweiler A, Reed DC, Holbrook SJ (2013) The importance of progressive senescence in the biomass dynamics of giant kelp (*Macrocystis pyrifera*). Ecology 94:1848–1858
Rosman JH, Koseff JR, Monismith SG, Grover J (2007) A field investigation into the effects of a kelp forest (*Macrocystis pyrifera*) on coastal hydrodynamics and transport. J Geophys Res 112:C02016
Rosman JH, Monismith SG, Denny MW, Koseff JR (2010) Currents and turbulence within a kelp forest (*Macrocystis pyrifera*): insights from a dynamically scaled laboratory model. Limnol Oceanogr 55:1145–1158
Schiel DR, Foster MS (2015) The biology and ecology of giant kelp forests. University of California Press, Oakland, CA
Shanks AL (2009) Pelagic larval duration and dispersal distance revisited. Biol Bull (Woods Hole) 216:373–385
Shepherd SA, Watson JE, Womersley HBS, Carey JM (2009) Long-term changes in macroalgal assemblages after increased sedimentation and turbidity in Western Port, Victoria, Australia. Bot Mar 52:195–206
Siegel DA, Kinlan BP, Gaylord B, Gaines SD (2003) Lagrangian descriptions of marine larval dispersion. Mar Ecol Prog Ser 260:83–96
Siegel DA, Mitarai S, Costello CJ, Gaines SD, Kendall BE, Warner RR, Winters KB (2008) The stochastic nature of larval connectivity among nearshore marine populations. Proc Natl Acad Sci USA 105:8974–8979
Stewart HL, Fram JP, Reed DC, Williams SL, Brzezinski MA, MacIntyre S, Gaylord B (2009) Differences in growth, morphology, and tissue carbon and nitrogen of *Macrocystis pyrifera* within and at the outer edge of a giant kelp forest in California, USA. Mar Ecol Prog Ser 375:101–112
Tait LW (2019) Giant kelp forests at critical light thresholds show compromised ecological resilience to environmental and biological drivers. Estuar Coast Shelf Sci 219:231–241
Tegner MJ, Dayton PK, Edwards PB, Riser KL (1997) Large-scale, low-frequency oceanographic effects on kelp forest succession: a tale of two cohorts. Mar Ecol Prog Ser 146:117–134
Traiger SB, Cohn B, Panos D, Daly M and others (2022) Limited biogeochemical modification of surface waters by kelp forest canopies: influence of kelp metabolism and site-specific hydrodynamics. Limnol Oceanogr 67: 392–403 doi:10.1002/lno.11999
Warton DI, Duursma RA, Falster DS, Taskinen S (2012) SMATR 3 — an R package for estimation and inference about allometric lines. Methods Ecol Evol 3:257–259
Watanabe H, Ito M, Matsumoto A, Arakawa H (2016) Effects of sediment influx on the settlement and survival of canopy-forming macrophytes. Sci Rep 6:18677
Zimmerman RC, Kremer JN (1986) *In situ* growth and chemical composition of the giant kelp, *Macrocystis pyrifera*: response to temporal changes in ambient nutrient availability. Mar Ecol Prog Ser 27:277–285

Editorial responsibility: Jean-Sébastien Lauzon-Guay, Dartmouth, Nova Scotia, Canada
Reviewed by: D. Schiel and 2 anonymous referees

Submitted: February 1, 2022
Accepted: June 15, 2022
Proofs received from author(s): August 3, 2022